



Facile synthesis of alumina-decorated multi-walled carbon nanotubes for simultaneous adsorption of cadmium ion and trichloroethylene



Jie Liang*, Junfeng Liu, Xingzhong Yuan*, Haoran Dong, Guangming Zeng, Haipeng Wu, Hou Wang, Jiayu Liu, Shanshan Hua, Shuqu Zhang, Zhigang Yu, Xiaoxiao He, Yan He

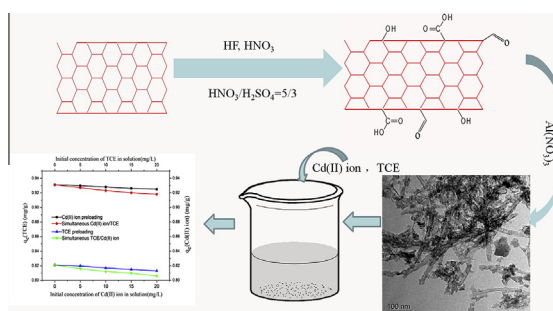
College of Environmental Science and Engineering, Hunan University, Changsha 410082, PR China

Key Laboratory of Environmental Biology and Pollution Control (Hunan University), Ministry of Education, Changsha 410082, PR China

HIGHLIGHTS

- Hybrid alumina-decorated multi-wall carbon nanotubes (MWCNTs) were synthesized.
- Alumina (Al_2O_3) was “soldered” by slow pyrolysis on MWCNTs.
- The hybrids were used to simultaneously remove Cd(II) ion and TCE from groundwater.
- The nanocomposites showed higher adsorption capacity than MWCNTs and Al_2O_3 .
- The Al_2O_3 could significantly restrain aggregation of functionalized MWCNTs.

GRAPHICAL ABSTRACT



ARTICLE INFO

Article history:

Received 16 January 2015

Received in revised form 11 March 2015

Accepted 12 March 2015

Available online 20 March 2015

Keywords:

Multi-walled carbon nanotubes

Alumina

Trichloroethylene

Cd(II) ion

Simultaneous adsorption

Groundwater

ABSTRACT

An adsorbent was prepared by decorating alumina onto the surface of multi-wall carbon nanotubes (MWCNTs) for simultaneous removal of cadmium ion (Cd(II) ion) and trichloroethylene (TCE) from groundwater. Structural characterization demonstrated that the nanocomposites was successfully synthesized and exhibited large surface area and restrained aggregation property. Batch experiments were conducted under various conditions (i.e., different pH, the presence of other groundwater constituents) to investigate the removal of Cd(II) ion or/and TCE by the alumina-decorated multi-walled carbon nanotubes ($\text{Al}_2\text{O}_3/\text{MWCNTs}$) and the underlying mechanisms. The adsorption kinetics of Cd(II) ion and TCE followed the pseudo-second-order kinetic model and exhibited 3-stage intraparticle diffusion mode. Equilibrium data of Cd(II) ion and TCE were best fitted by Langmuir and Freundlich model, respectively. The adsorption mechanisms of $\text{Al}_2\text{O}_3/\text{MWCNTs}$ toward Cd(II) ion and TCE mainly involved in the electrostatic interactions, the hydrogen bond interactions and the protonation or hydroxylation of Al_2O_3 . The maximum adsorption capacities of $\text{Al}_2\text{O}_3/\text{MWCNTs}$ for TCE and Cd(II) ion were 19.84 mg/g and 27.21 mg/g, respectively, which were higher than that of Al_2O_3 , MWCNTs and the functionalized MWCNTs. The results suggested that the $\text{Al}_2\text{O}_3/\text{MWCNTs}$ could be considered as an effective and promising adsorbent for simultaneous removal of Cd(II) ion and TCE from groundwater.

© 2015 Elsevier B.V. All rights reserved.

1. Introduction

Groundwater pollution has become a critical environmental and economic issue in the worldwide [1]. Heavy metal ions such as cadmium ion (Cd(II) ion) are the main contaminant of groundwater and soils at the metal plating industry and the solid waste

* Corresponding authors at: College of Environmental Science and Engineering, Hunan University, Changsha 410082, PR China. Tel.: +86 731 88821413; fax: +86 731 88823701.

E-mail addresses: liangjie@hnu.edu.cn, liangjie82@163.com (J. Liang), yxz@hnu.edu.cn (X. Yuan).

landfill site [1]. Due to its nonbiodegradable nature, Cd(II) ion can accumulate in the environment and enter the food chain, causing adverse effects to human health and ecological receptors and resulting in osteoporosis, anemia and renal damage [2]. Because of the improper storage and disposal of the spent solvents, groundwater contamination by chlorinated solvents (mainly trichloroethylene) at many industries and solid waste landfill sites has been discovered and can influence the human central nervous system, causing symptoms such as dizziness, headaches, confusion, euphoria, facial numbness, and weakness [3,4]. Therefore, the US EPA recommends permissible limit in drinking water to be 5 $\mu\text{g/L}$ for both Cd(II) ion and TCE [5,6]. It should be noted that there is a high possibility that Cd(II) ion and TCE coexist in the environment, such as groundwater contaminated by the landfill leachate [7,8]. Thus, there is a need to find an effective approach to remove the excess Cd(II) ion and TCE from groundwater simultaneously.

Several methods have been applied for the removal of Cd(II) ion or TCE from aqueous solution, e.g., precipitation, ion exchange, coagulation, and adsorption [9]. Among these methods, adsorption is one of the most popular and widely used techniques for groundwater deputation, and shows a robust operating configuration, high reliability and economic advantages [10]. Various adsorbents like magnetic mesoporous carbon [11], carbon [2], activated alumina [12], activated carbon [13], sustainable organic mulch [10], acid/basic oxygen furnace slag [3], pine needle biochars [14] were used for the removal of Cd(II) ion/TCE. However, many of these adsorbents have low adsorption capacity and slow process kinetics. Hence, it is quite necessary to develop some useful adsorbents.

Carbon nanotubes (CNTs), including single-wall (SWCNTs) and multi-wall (MWCNTs), have attracted significant attention in environmental protection. Unlike many adsorbents, MWCNTs possess different features that contribute to the excellent removal capacities; such as fibrous shape with high aspect ratio, large accessible external surface area, light mass density, easily modified surfaces and well developed mesopores [15–17]. However, the strong intermolecular interactions between the tubes can lead to the formation of aggregates, decreasing their accessible surface area and hindering the application of MWCNTs [18]. In order to solve this problem, the uses of MWCNTs as support of CeO_2 [19], iron oxides [20], TiO_2 [21], tungsten oxide [22], chitosan [23], cellulose [24], graphene [25] and MnO_2 [26] have been reported. Saleh et al. [27] synthesized the nanocomposite MWCNT/alumina via hydrothermal treatment and investigated the possible chemical bond formation between functionalized carbon nanotubes and alumina. Previous studies also synthesized the amorphous alumina supported on carbon nanotubes, the granular carbon nanotubes/alumina hybrid and the nanofloral clusters of carbon nanotubes/activated alumina to remove fluoride and lead [9,28], diclofenac sodium and carbamazepine [29] and Cr(VI) and Cd(II) ion [12], respectively. This composites not only possess large surface area, a better orientation degree [30], but also exhibit excellent characteristics and high adsorption capacities for contaminants. But most current researches focused on the adsorption of heavy metal or organic contaminants and failed to consider the potential interactions between heavy metal and organic contaminants in a coexisting system. To the best of our knowledge, there are no reports about the synthesis of nano-sized $\text{Al}_2\text{O}_3/\text{MWCNTs}$ composites and its application in the simultaneous removal of Cd(II) ion and TCE from groundwater.

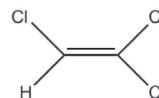
In the present work, we synthesized a new $\text{Al}_2\text{O}_3/\text{MWCNTs}$ adsorbent with an improved approach and investigated the feasibility and mechanisms of simultaneous adsorption of Cd(II) ion and TCE from contaminated groundwater. The influences of solution pH and groundwater constituents on the adsorption properties were evaluated. The kinetics of Cd(II) ion and TCE adsorption were analyzed using a pseudo-second-order kinetic model. The

adsorption equilibrium was analyzed using Langmuir and Freundlich models. The effects of Cd(II) ion on the sorption of TCE and vice versa were also investigated. Finally, the feasibility of $\text{Al}_2\text{O}_3/\text{MWCNTs}$ for Cd(II) ion and TCE removal was examined in the synthetic groundwater to simulate the situation in the practical application.

2. Materials and methods

2.1. Materials

MWCNTs (purity: >95 wt%; ash: <1.5 wt% outer diameter: 10–20 nm; length: 10–30 μm) were purchased from Chengdu Organic Chemistry Co. Ltd, Chinese Academy of Sciences. TCE was purchased from Sigma–Aldrich Chemical Co, and used directly as received. Different initial concentrations of Cd(II) ion solutions were prepared by dissolving $\text{Cd}(\text{NO}_3)_2 \cdot 5\text{H}_2\text{O}$ in ultrapure water. The initial TCE solution was prepared by dilution of the TCE-in-methanol mixture. Stock solutions were prepared daily. Glassware was kept overnight in a 10% (v/v) HNO_3 solution. The synthetic groundwater containing 230 mg/L Na^+ , 32 mg/L Ca^{2+} , 234 mg/L Cl^- , 183 mg/L HCO_3^- , 96 mg/L SO_4^{2-} was used as the background electrolyte in this study, which was within the typical concentrations of natural groundwater [31].



The chemical structure of TCE

2.2. Synthesis of $\text{Al}_2\text{O}_3/\text{MWCNTs}$

The preparation of $\text{Al}_2\text{O}_3/\text{MWCNTs}$ was accomplished according to the previous literature with some modification [9,29]. All glassware was cleaned by aqua regia freshly prepared prior to use. The purification of the MWCNTs was accomplished by adding 2.5 g MWCNTs into 50 mL concentrated nitric acid (67% by weight) at 70 $^\circ\text{C}$ for 24 h, followed by filtering and washing with ultrapure water, and then adding into 50 mL HF (40% by weight) at 70 $^\circ\text{C}$ for 24 h. After that, the turbid liquid was filtered and washed with ultrapure water until the pH approach 7.0, and then drying at 105 $^\circ\text{C}$ for 6 h. Then, the purified MWCNTs were functionalized by refluxing with nitric acid (67% by weight) and sulfuric acid (96% by weight) (volume ratio 5:3) [32] at 140 $^\circ\text{C}$ for 2 h under stirring conditions (50 rpm). The product was filtered and rinsed with ultrapure water until the pH approach 7.0, coupled with drying overnight in the oven. Typically, 2.5 g functionalized MWCNTs were dispersed into ultrapure water and magnetically agitated 6 h at which acceptable level of dispersion was observed. Afterwards, 7.835 g $\text{Al}(\text{NO}_3)_3 \cdot 9\text{H}_2\text{O}$ was properly dissolved in ultrapure water. The $\text{Al}(\text{NO}_3)_3$ solutions were drop wise added into dispersed functionalized MWCNTs. During consecutive drops, appropriate time should be left for the aluminum to reach, appropriately disperse and engage to the surface of functionalized MWCNTs. After that, the suspension was dried at 105 $^\circ\text{C}$. The obtained material was heated up to 400 $^\circ\text{C}$ for 2 h, where the pyrolysis process resulted in the alumina formation decorated onto the surface of functionalized MWCNTs, and sealed in glass containers for subsequent testing.

2.3. Characterization methods

The morphologies and sizes of the $\text{Al}_2\text{O}_3/\text{MWCNTs}$ were analyzed by the S-4800 field emission scanning electron microscope

(FESEM, Hitachi, Japan) and the transmission electron microscopy (TEM) using a JEOL-1230 electron microscopy. The BET specific surface areas were determined by Belsorp-Mini II analyser (Japan), pore size distribution and the total pore volume were derived from the desorption branches of the isotherms based on BJH model. The crystal phases of the samples were determined by X-ray diffractometer with Cu-K radiation (XRD, M21X, MAC Science Ltd., Japan). Infrared absorption spectra were measured at room temperature on a FTIR spectrometer (Nicolet Instrument Corporation, USA).

2.4. Adsorption experiments

Batch adsorption experiments of Cd(II) ion (or TCE) were all conducted in 100 mL conical flasks (or 50 mL Teflon-lined screw-capped glass-vials with no headspace to minimize the volatile loss of TCE) at 150 rpm (Fig. S1) at 25 ± 1 °C [26]. The equilibrium time for Cd(II) ion/TCE adsorption was 4 h/24 h. The doses of Al₂O₃/MWCNTs were 1 g/L (Fig. S2). The influence of solution pH values on Cd(II) ion/TCE removal was studied by adding Al₂O₃/MWCNTs into the conical flasks/glass-vials containing 50 mL of 1 mg/L Cd(II) ion/TCE solution [33] with pH values ranging from 4.0 to 10.0. The pH values of the solutions were adjusted with 0.1 M NaOH or 0.1 M HCl. The effect of contact time on the adsorption of Cd(II) ion/TCE by Al₂O₃, MWCNTs, functionalized MWCNTs and Al₂O₃/MWCNTs was also conducted in conical flasks/glass-vials containing 50 mg of the adsorbent and 50 mL of 1 mg/L Cd(II) ion/TCE at pH 7.0. The samples were taken using a pipette at predetermined time intervals (0–16 h and 0–48 h). Adsorption isotherms experiments were performed in conical flasks/glass-vials containing 50 mL Cd(II) ion/TCE solution of different concentrations (varying from 0.1 to 64 mg/L) at pH 7.0. Competitive adsorption studies were conducted when both adsorbates were adsorbed onto Al₂O₃/MWCNTs simultaneously or one of them was preloaded at pH 7.0. In the simultaneous adsorption experiments, the concentration of TCE/Cd(II) ion was fixed at 1 mg/L while the concentration of Cd(II) ion/TCE varied from 0 to 20 mg/L. In the preloading studies, TCE/Cd(II) ion was first adsorbed onto Al₂O₃/MWCNTs and then different concentrations of Cd(II) ion/TCE solutions (0–20 mg/L) were added for further adsorption. A series of concentrations of CaCl₂ (0–80 mg/L) or humic acid (0–20 mg/L) were added to the system to study the effect of groundwater constituents, which was within the typical range in natural groundwater [34]. Finally, the practical application was simulated in glass-vials containing 50 mL of 1 mg/L Cd(II) ion and TCE. The Cd(II) ion and TCE stock solution was prepared using ultrapure water and synthetic groundwater. The pH = 7.6 of these solutions was not adjusted to simulate the real situation in practical application.

2.5. Analysis

To assure the accuracy, reliability, and reproducibility of the collected data, all batch tests were performed in triplicate. The data analysis was carried out using standard deviation and the average relative error (ARE%) (Table S1). Blank tests without sorbent addition showed that the losses resulting from volatilization, sorption on reactor walls were less than 4% (Table S2). After reaction, the Al₂O₃/MWCNTs solids were filtered by 0.22 μm glass-fiber filter. Cd(II) ion concentrations were determined by a Perkin-Elmer Analyst 700 atomic absorption spectrophotometer (AAS, Perkin-Elmer, USA) [35]. While the TCE concentrations were measured by a gas chromatograph (Agilent, GC 6890) equipped with an electron capture detector (ECD) and a Purge & Trap system (Tekmar LSC-2000) [10]. The amounts of adsorbed Cd(II) ion and TCE were determined by the difference between initial and final equilibrium concentrations.

3. Results and discussion

3.1. Characterization

As shown in the TEM image (Fig. 1a), tangled MWCNTs possess a diameter of about 25 nm in the dissolved solutions. Fig. 1b showed that the functionalized MWCNTs did not change significantly comparing with MWCNTs. This indicates that the functionalization with severe and harsh experimental conditions did not alter the nanotube structure [36]. However, it was noticeable that there were more identifiable bright patches on functionalized MWCNTs than MWCNTs, suggesting the functionalization created defect sites and polar groups, such as hydroxyl, carbonyl and carboxyl groups (as shown in Fig. 3), which could interact with Al₂O₃ nanoparticles through the hydrogen bonding [29,37]. From Fig. 1c and d, it can be observed that the functionalized MWCNTs were decorated by Al₂O₃ nanoparticles. The EDAX measurements (Fig. 1e) shows three components presented in the nanocomposite: carbon, oxygen, aluminum. TGA further indicates the percent of functionalized MWCNTs in the Al₂O₃/MWCNTs was around 45 wt% (Fig. S3).

Fig. 2 displays the XRD patterns of the MWCNTs, functionalized MWCNTs and Al₂O₃/MWCNTs. The two peaks at 26.0°, 42.7° are identified as the MWCNTs and the other diffraction peaks (53.5°, 44.0°) can be indexed to the planes of hexagonal graphite structure in the Fig. 2a and b [38]. Moreover, the broad peaks of the Fig. 2b were higher intensity than Fig. 2a, indicating functionalized MWCNTs was smaller than MWCNTs [39]. In Fig. 2c, the diffraction peaks of both functionalized MWCNTs and alumina can be observed. The main dominant peaks for Al₂O₃ were identified at $2\theta = 18.2^\circ, 20.0^\circ, 37.5^\circ, 40.0^\circ, 64.5^\circ, 67.4^\circ$ [9,27]. The two peaks (26.0°, 42.7°) reflected MWCNTs in Al₂O₃/MWCNTs are much lower than that of functionalized MWCNTs. This is due to the lower XRD intensity of MWCNTs compared with the crystalline Al₂O₃, these peaks of functionalized MWCNTs are nearly masked [27]. The result further confirmed the functionalized MWCNTs were decorated by Al₂O₃ nanoparticles.

FTIR spectroscopic analysis of MWCNTs, functionalized MWCNTs and Al₂O₃/MWCNTs were depicted by Fig. 3. For three materials, the bands spectrum at 1180 cm⁻¹ were assigned to the stretching vibration of C–O from phenol or lactone groups and C–C bonds [40]. The peak at around 1580 cm⁻¹ could be assigned to the C=C stretch of the aromatic [27]. Those peaks at 3400–3465 cm⁻¹ corresponded to –OH groups, indicating the existence of the hydroxyl groups on the surface of materials or the adsorption of some atmospheric water during FTIR measurements [9], which become sharper in functionalized MWCNTs. That was because the functionalization introduced various functional groups onto their surfaces [37]. Meanwhile, the lower intensity of the peaks (3400–3465 cm⁻¹) of Al₂O₃/MWCNTs comparing to functionalized MWCNTs was probably ascribed to the alumina located at the sidewalls of the functionalized MWCNTs through the hydrogen bond between Al–OH and carboxyl groups [12]. The two peaks at 2920 and 2854 cm⁻¹ corresponding to the C–H stretch vibration, which become weak in Fig. 3b, suggesting the surface of functionalized MWCNTs has been decorated by alumina [9]. For functionalized MWCNTs, the adsorption peak at 1710 cm⁻¹ corresponding to the stretching vibration of C=O from –COOH. But in the Al₂O₃/MWCNTs, the peak assigned to C=O stretching vibration is shifted from 1710 to 1630 cm⁻¹, this shift suggests that the carboxylic acid groups on the functionalized MWCNTs are involved in an interaction with the alumina. This illustrates that carboxylic acid groups on the surface of functionalized MWCNTs and hydroxyl groups on alumina interacts with each other via esterification to form the chemical bond [27]. The adsorption band

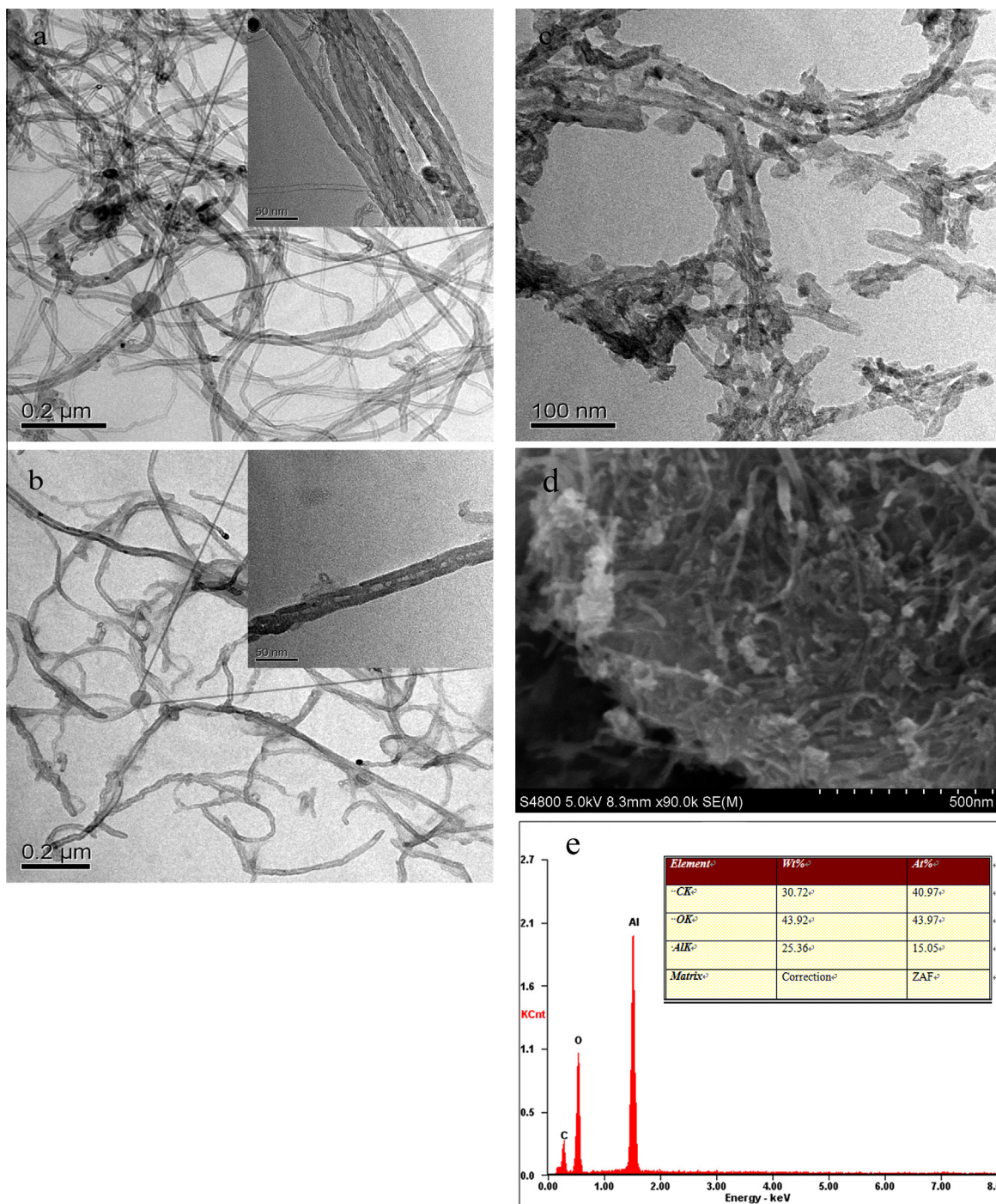


Fig. 1. TEM photograph of MWCNTs (a), functionalized MWCNTs (b) and TEM (c), SEM (d), EDAX (e) of Al₂O₃/MWCNTs.

at around 500 cm⁻¹ in Fig. 3b reveals the vibrational properties of Al–O band, which is obviously caused by the existence of alumina [27].

The BET of MWCNTs (a), functionalized MWCNTs (b), Al₂O₃/MWCNTs (c) and BJH (d) are shown in Fig. S4. The corresponding pore size distribution showed that the main and mean pore diameter of MWCNTs and functionalized MWCNTs centered at 1.0–10.0 nm and 11.475, 9.769 nm, respectively (Table 1). It could be seen that the oxidation had no noticeable effects on pore size distributions, but reduced the mean diameter of functionalized MWCNTs, which might be attributed to the removal of the amorphous carbon from the surface [41]. However, for Al₂O₃/MWCNTs,

the mean pore diameter was 10.979 nm. It could be ascribed to their wide polydispersity, entanglement and an open network of micropores with a pore size distribution from 1.0 to 16.0 nm [42].

3.2. Effect of pH and underlying mechanism

The removal of Cd(II) ion and TCE as a function of pH was shown in Fig. 4. The amounts of Cd(II) ion adsorbed onto Al₂O₃/MWCNTs increased slightly over the pH range of 4.0–6.0, but experienced a rapid rise at pH 6.0–7.0. This trend was similar to Gupta et al. [43,44] reported. At pH < pHPzc = 6.2 (Fig. S5), the surfaces of Al₂O₃/MWCNTs having a net positive charge hinder the Cd(II) ion

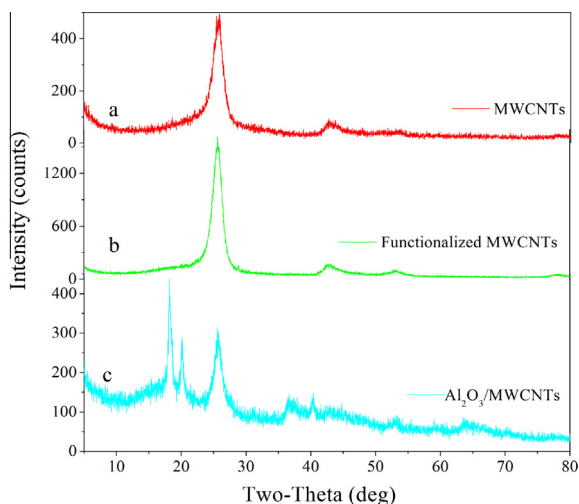


Fig. 2. XRD patterns of MWCNTs (a), functionalized MWCNTs (b) and $\text{Al}_2\text{O}_3/\text{MWCNTs}$ (c).

adsorption due to the electrostatic repulsion. Also, stiff competitions between H^+ and $\text{Cd}(\text{II})$ ion for the active sites will also decrease the $\text{Cd}(\text{II})$ ion adsorption [43]. At $\text{pH} > \text{pH}_{\text{pzc}}$, hydroxyl groups were progressively deprotonated and a net negative charge was presented on the surfaces of $\text{Al}_2\text{O}_3/\text{MWCNTs}$, which contributed to the $\text{Cd}(\text{II})$ ion adsorption through the formation of metal–ligand composite complexes with cationic $\text{Cd}(\text{II})$ ion [45]. Over the pH range of 8.0–10.0, the adsorption capacity of $\text{Cd}(\text{II})$ ion increased from 0.961 to 0.973 mg/g, which was attributed to the critical pH value for $\text{Cd}(\text{II})$ ion hydrolysis (formation of $\text{Cd}(\text{OH})^+$ and $\text{Cd}_2(\text{OH})_2^{2+}$) and precipitation ($\text{Cd}(\text{OH})_2 \geq 8.0$) through the electrostatic interaction and deposition [46]. Meanwhile, the electrostatic attraction between the pairs of electrons on the oxygen atoms of alumina and the positive cationic $\text{Cd}(\text{II})$ ion also facilitated the adsorption of $\text{Cd}(\text{II})$ ion [9]. Moreover, surface precipitation and complexation between the carboxylic group, hydroxyl and $\text{Cd}(\text{II})$ ion also contributed to the adsorption of $\text{Cd}(\text{II})$ ion [47]. Finally, the physical property of the $\text{Al}_2\text{O}_3/\text{MWCNTs}$ and the van der Waals interactions occurring between the hexagonally arrayed carbon atoms in the graphite sheet and $\text{Cd}(\text{II})$ ion could also conduce to the adsorption of $\text{Cd}(\text{II})$ ion [47].

Unlike the $\text{Cd}(\text{II})$ ion, TCE was a non-ionic and lipophilic substance. Therefore, the electrostatic interaction had little effect on

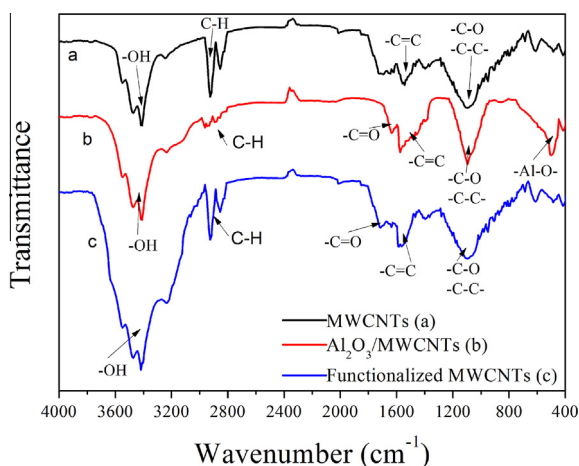


Fig. 3. FTIR spectra of MWCNTs (a), $\text{Al}_2\text{O}_3/\text{MWCNTs}$ (b) and functionalized MWCNTs (c).

Table 1

Pore structure parameters of MWCNTs, functionalized MWCNTs and $\text{Al}_2\text{O}_3/\text{MWCNTs}$.

Sample	S_{BET} (m^2/g)	V_p (cm^3/g)	Mean pore diameter (nm)
MWCNTs	74.21	0.3154	11.457
Functionalized MWCNTs	115.66	0.3042	9.769
$\text{Al}_2\text{O}_3/\text{MWCNTs}$	109.82	0.2492	10.979

S_{BET} , BET surface area; V_p , pore specific volume.

TCE adsorption. It could be verified by the fact that the adsorption of TCE had no significant change below and over the isoelectric point (Fig. 4) [48]. These results are consistent with findings of previous studies, which suggested that pH should not affect the adsorption of TCE [3,5,10,13,14]. The slightly increased adsorption of TCE with the pH increasing from 3.0 to 10.0 could be ascribed to the $-\text{Al}-\text{OH}_2^+$ and $-\text{Al}-\text{OH}$ groups formed by the protonation or hydroxylation of Al_2O_3 , which facilitated the adsorption of TCE through the hydrogen bonds [29,41]. Because TCE was a planar molecule having a diameter of 0.56 nm [14], the lower-size micropores of $\text{Al}_2\text{O}_3/\text{MWCNTs}$ had stronger adsorption energies due to more contact with TCE, thus would be preferentially occupied if the pores were not small enough to cause molecular sieving [49]. Meanwhile, the van der Waals forces could facilitate the intermolecular attraction between TCE and $\text{Al}_2\text{O}_3/\text{MWCNTs}$ regardless of the TCE molecular size, electric charge and polarizability [41]. Besides, the π - π bonding also takes place between bulk π system of MWCNTs and TCE molecules with $\text{C}=\text{C}$ [16]. Lastly, the sidewall of MWCNTs has highly hydrophobic property because of high π electron density of sp^2 carbons and TCE can interact with the side wall of MWCNTs through the hydrophobic interactions [17,36]. A schematic presentation of $\text{Cd}(\text{II})$ ion and TCE interaction with $\text{Al}_2\text{O}_3/\text{MWCNTs}$ was shown in Fig. 5.

3.3. Adsorption kinetics

Fig. 6 shows the time dependent data of $\text{Cd}(\text{II})$ ion and TCE adsorption by Al_2O_3 , MWCNTs, functionalized MWCNTs and $\text{Al}_2\text{O}_3/\text{MWCNTs}$. For $\text{Al}_2\text{O}_3/\text{MWCNTs}$, the equilibrium for $\text{Cd}(\text{II})$ ion and TCE was achieved within 4 h and 24 h, respectively. The pseudo-second-order kinetic model were used to investigate the adsorption kinetics [50,51], with the parameters calculated and listed in Table 2. The pseudo-second-order model shows a linear relationship with very excellent correlation coefficients ($R^2 \geq 0.999$) and good agreement between experimental ($q_{e,\text{cal}}$) and calculated ($q_{e,\text{exp}}$) values for both contaminant adsorption.

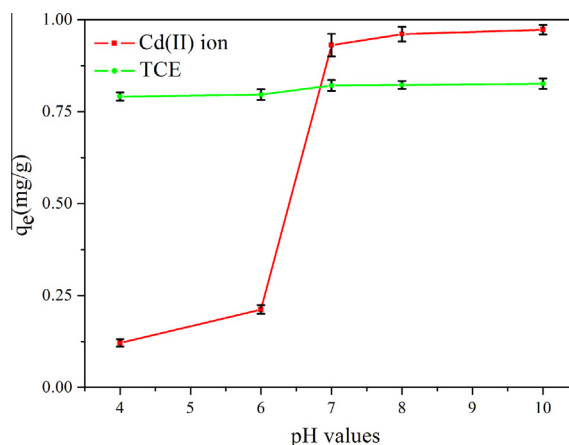


Fig. 4. Effect of pH on the adsorption of $\text{Cd}(\text{II})$ ion and TCE by $\text{Al}_2\text{O}_3/\text{MWCNTs}$.

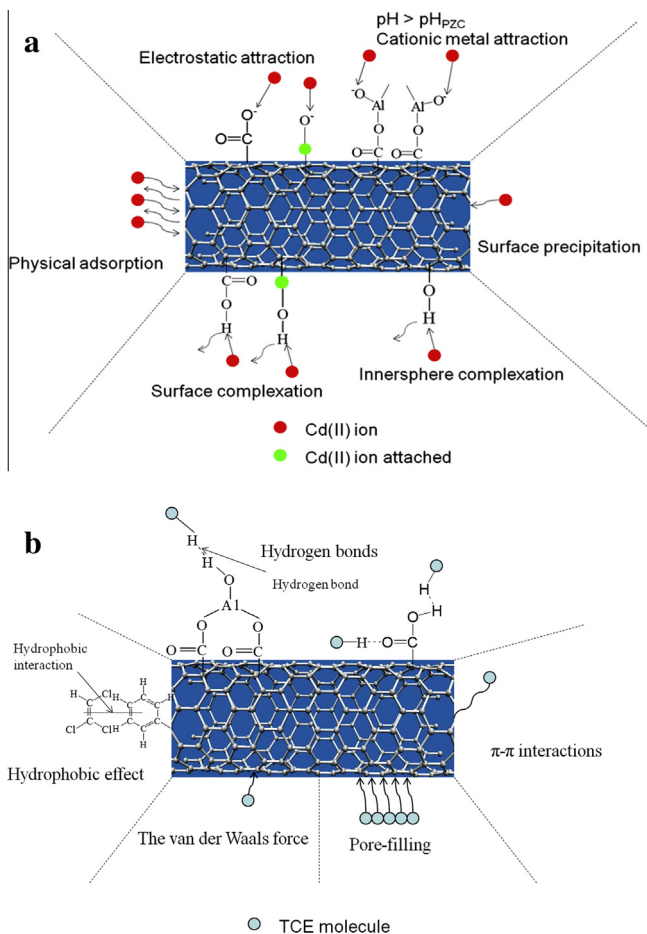


Fig. 5. The schematic presentation of Cd(II) ion (a) and TCE (b) interaction with $\text{Al}_2\text{O}_3/\text{MWCNTs}$.

Thus, the adsorption rates of $\text{Al}_2\text{O}_3/\text{MWCNTs}$ were controlled by physical force while the chemisorption played a small role due to the functional groups such as $-\text{COOH}$ and $-\text{OH}$ [17]. The rate constant of Cd(II) ion was relatively higher than that of TCE, indicating that the uptake of Cd(II) ion was faster than TCE.

To further evaluate the mechanism and the rate-controlling steps affecting the adsorption kinetics, intraparticle diffusion model (Fig. 6c) has been applied to investigate the adsorption process. The intraparticle diffusion constants were calculated and listed in Table 2. As shown in Fig. 6c and Table 2, the plots for adsorption of Cd(II) ion and TCE by $\text{Al}_2\text{O}_3/\text{MWCNTs}$ were found to be multi-linear and the order of adsorption rate was $k_{id,1} > k_{id,2} > k_{id,3}$. At the initial stage, Cd(II) ion and TCE were adsorbed on the exterior surface of $\text{Al}_2\text{O}_3/\text{MWCNTs}$. The instantaneous diffusion period (slope $k_{id,1}$) revealed that there was a strong adsorption occurred between the external surfaces of $\text{Al}_2\text{O}_3/\text{MWCNTs}$ and Cd(II) ion/TCE, which was attributed to the electrostatic attractive forces and the SSA ($109.82 \text{ m}^2/\text{g}$) of $\text{Al}_2\text{O}_3/\text{MWCNTs}$ [37]. Meanwhile, the intra-particle diffusion rate constant of Cd(II) ion ($k_{id,1} = 0.8912$) > that of TCE ($k_{id,1} = 0.3919$) indicated the adsorption of the Cd(II) ion was more easy than TCE at the initial stage. With Cd(II) ion and TCE entering into the micropores of $\text{Al}_2\text{O}_3/\text{MWCNTs}$, the lower-size micropores would be preferentially occupied [49], and then the diffusion resistance increased, leading to the decrease of diffusion rates ($k_{id,2}$). Finally, the insignificant rise ($k_{id,3}$) indicated that the Cd(II) ion and TCE traveled into the innermost surfaces of $\text{Al}_2\text{O}_3/\text{MWCNTs}$ and reached the equilibrium period [51]. In this process, a small amount of adsorption occurred on the exterior surface [45]. According to this study, we could know the adsorption trends of

the Cd(II) ion and TCE were almost the same, which were consistent with the previous works [3,13,35,37,52].

For $\text{pH} = 7.0$, the zeta potentials followed the order $\text{Al}_2\text{O}_3 > \text{Al}_2\text{O}_3/\text{MWCNTs} > \text{MWCNTs} > \text{functionalized MWCNTs}$ (Fig. S5). The point of zero charge of functionalized MWCNTs was very close to the oxidized MWCNTs reported in other literature [15]. Therefore, the adsorption capacity of Cd(II) ion should follow the order functionalized MWCNTs > MWCNTs (0.4157 mg/g) > $\text{Al}_2\text{O}_3/\text{MWCNTs}$ > Al_2O_3 (0.6817 mg/g) due to the electrostatic forces. But the adsorption capacity of $\text{Al}_2\text{O}_3/\text{MWCNTs}$ (0.9310 mg/g) was greater than that of functionalized MWCNTs (0.9113 mg/g) from Table S1 and Fig. S6. It was attributed to the role of Al_2O_3 , which could significantly restrain aggregation of functionalized

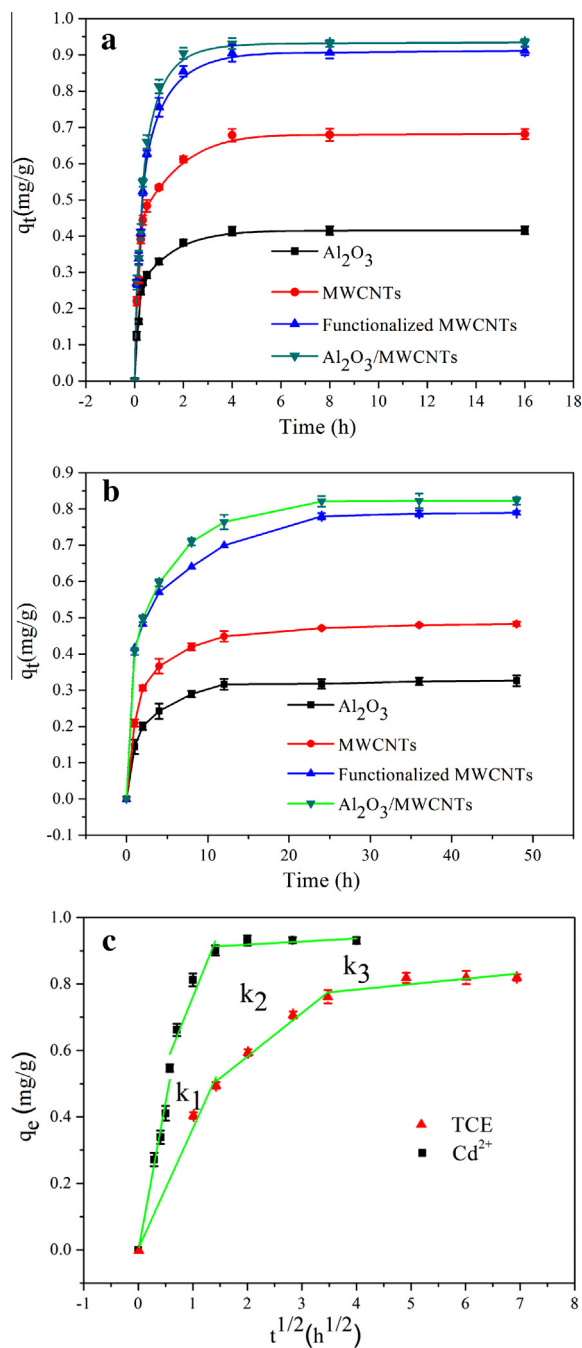


Fig. 6. Effect of contact time on the adsorbed amount of Cd(II) ion (a), TCE (b) by Al_2O_3 , MWCNTs, functionalized MWCNTs, $\text{Al}_2\text{O}_3/\text{MWCNTs}$ and the intraparticle diffusion model (c) of Cd(II) and TCE adsorption by $\text{Al}_2\text{O}_3/\text{MWCNTs}$.

Table 2
Summary of models and best-fit parameters of the sorption kinetics and isotherms (Al₂O₃/MWCNTs).

Adsorbate	Model ^a	Parameter 1	Parameter 2	Parameter 3	Parameter 4	Parameter 5	Parameter 6
Cd(II) ion	Pseudo-second-order ($t/q_t = 1/kq_e^2 + t/q_e$)	$K = 5.7644$	$q_e^a = 0.9310$	$q_e^b = 0.9480$	$R^2 = 0.9996$	ARE (%) = 1.87	
	Intraparticle diffusion ($q_t = k_{id}t^{1/2}$)	$k_{id,1} = 0.8912$	$R^2 = 0.9753$	$k_{id,2} = 0.4071$	$R^2 = 0.8871$	$k_{id,3} = 0.0091$	$R^2 = 0.6762$
	Langmuir ($q_e = q_m K_L C_e / (1 + K_L C_e)$)	$K_L = 0.03983$	$q_m = 27.21$	$R^2 = 0.9972$			
	Freundlich ($q_e = K_F C_e^{1/n}$)	$K_F = 2.0678$	$n = 1.8104$	$R^2 = 0.9830$			
TCE	Pseudo-second-order	$K = 1.1048$	$q_e^a = 0.8220$	$q_e^b = 0.8430$	$R^2 = 0.9990$	ARE (%) = 2.53	
	Intraparticle diffusion	$k_{id,1} = 0.3619$	$R^2 = 0.9728$	$k_{id,2} = 0.1306$	$R^2 = 0.9770$	$k_{id,3} = 0.0163$	$R^2 = 0.5559$
	Langmuir	$K_L = 0.03312$	$q_m = 19.84$	$R^2 = 0.9925$			
	Freundlich	$K_F = 1.294$	$n = 1.742$	$R^2 = 0.9936$			

^a The measured adsorption capacity at equilibrium.

^b The calculated adsorption capacity at equilibrium. ARE (%) is the average relative error.

^{*} k (g/mg h) and k_{id} (mg/g h^{1/2}) are the pseudo-second-order and intra-particle diffusion rate constant, q_t and q_e are the adsorbed amount of adsorbent at time t and at equilibrium, respectively (mg/g), q_m (mg/g) is the maximum adsorption capacity, C_e (mg/L) is the equilibrium solute concentration, K_L (L/mg) is the Langmuir constant related to adsorption energy, K_F and n are Freundlich constants and intensity factors, respectively.

MWCNTs in the aqueous environment [9]. But for TCE, the SSA followed the order functionalized MWCNTs (115.66 m²/g) > Al₂O₃/MWCNTs (109.82 m²/g) > MWCNTs (74.21 m²/g) (Table 1). Because the large SSA of the adsorbents could facilitate the adsorption of TCE, the adsorption capacity of TCE should follow the order functionalized MWCNTs > Al₂O₃/MWCNTs > MWCNTs (0.4823 mg/g). But the adsorption capacity of Al₂O₃/MWCNTs (0.8220 mg/g) was preponderant when compared with functionalized MWCNTs (0.7893 mg/g). That was because the functionalized MWCNTs easily reunite than Al₂O₃/MWCNTs in the aqueous solution [30]. Meanwhile, the hydrogen bond between Al–OH and carboxyls reduced the functional groups of the functionalized MWCNTs in the Al₂O₃/MWCNTs and facilitated the adsorption of TCE through the hydrophobic interactions.

3.4. Adsorption isotherms

The nonlinear Langmuir and Freundlich adsorption isotherms of Cd(II) ion/TCE on Al₂O₃/MWCNTs were presented in Fig. 7. The results were summarized in Table 2. From the Table 2, the Freundlich isotherm model of TCE shows the higher correlation coefficient ($R^2 = 0.9936$) than the Langmuir model ($R^2 = 0.9925$). Since heterogeneous adsorption on adsorbents is assumed in Freundlich model, better fitting with this model might suggest that the existence of the heterogeneous distribution on the surfaces or pores of Al₂O₃/MWCNTs [48,53,54]. According to other study, the internal sites, interstitial channels, external grooves and exposed

surface sit of Al₂O₃/MWCNTs were all the adsorption sites of TCE [17]. Value of $1/n$ (<1.0) gave an indication of the favorability of TCE adsorption by Al₂O₃/MWCNTs [55]. The results were consistent with the previous works, such as iron oxide nanoparticles [56], activated carbon [13]. However, the correlation coefficient indicated the adsorption of Cd(II) ion tended to be fitted better by the Langmuir model (Table 2). Better fitting with this model might suggest the existence of homogeneous active sites of Cd(II) ion on Al₂O₃/MWCNTs [11]. The results were consistent with the Al₂O₃ and CNTs [35,57]. The dimensionless constant ($R_L = 1/(1 + K_L C_0)$) called the separation factor was used to further analyze Langmuir model, where K_L (L/mg) is the Langmuir constant and C_0 (mg/L) is the initial Cd(II) ion concentration. The R_L ranged from 0.2818 to 0.9960 for Al₂O₃/MWCNTs signified that the adsorption of Cd(II) ion was favorable [58].

As shown in Table 2, the estimated maximum TCE adsorption capacity of Al₂O₃/MWCNTs was 19.84 mg/g, which was preponderant when compared with adsorbents such as allophane–TiO₂ composite (2.52 mg/g) [59], multiwall carbon nanotubes (2.75 mg/g) [52], granular activated carbon (2.8 mg/g) [60] and was comparable to that of activated carbon (23.46 mg/g) [13]. Meanwhile, the estimated maximum Cd(II) ion adsorption capacity of Al₂O₃/MWCNTs was 27.21 mg/g, which was much higher than that of other adsorbents such as nano-alumina on SWCNT (2.18 mg/g) [61], carbon nanotubes (HNO₃) (2.92 mg/g) [47], aluminum oxide nanoparticles (8.25 mg/g) [57], multi-walled carbon nanotubes (H₂SO₄) (8.7 mg/g) [37], carbon nanotube on micro-sized Al₂O₃ (12 mg/g) [62], CNT (amino-functionalization) (25.7 mg/g) [63].

3.5. Competitive adsorption studies

According to Fig. 8, the adsorption capacity of TCE reduced with the increasing Cd(II) ion concentrations in the simultaneous adsorption studies, which suggested that Cd(II) ion could inhibit TCE adsorption. Two mechanisms might be involved in this fact. Firstly, Cd(II) ion could form complexation with acidic functional groups. The complexation hindered the TCE molecule access to the surfaces of Al₂O₃/MWCNTs [64]. Secondly, Cd(II) ion could easily compete with water molecules for functional groups on Al₂O₃/MWCNTs surface to form strong inner-sphere complexes. The complexed heavy metal ions were likely to host one or more hydration shells of dense water, which intruded adjacent Al₂O₃/MWCNTs surfaces and competed with TCE for surface area, leading to Cd(II) ion inhibition on TCE adsorption in the local region around the metal-complexed moieties [49]. For TCE-preloading experiments, little TCE was desorbed at higher concentration of Cd(II) ion, which showed that Cd(II) ion could compete with TCE for the same adsorption energies again.

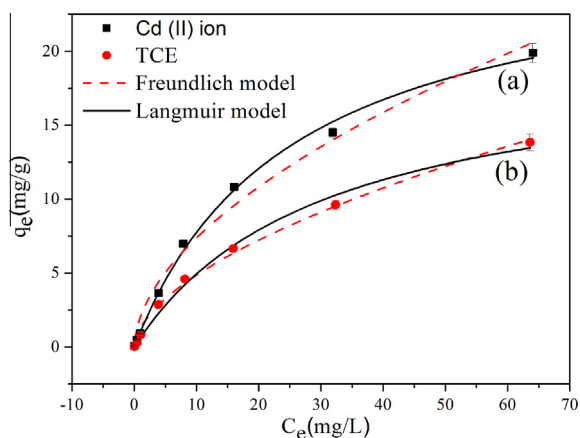


Fig. 7. Comparison of the experimental data and model fits of the Langmuir and Freundlich isotherms for the adsorption of Cd(II) ion (a) and TCE (b) by Al₂O₃/MWCNTs.

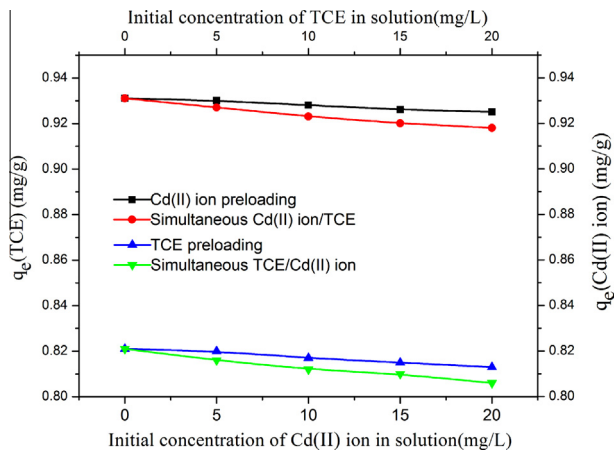


Fig. 8. Effects of simultaneous adsorption and TCE (Cd(II) ion) preloading on the sorption capacity of $\text{Al}_2\text{O}_3/\text{MWCNTs}$ for TCE (Cd(II) ion).

For Cd(II) ion, different concentrations of TCE had a relatively small suppression effect on the sorption of Cd(II) ion in the simultaneous adsorption studies and Cd(II) ion-preloading experiments. The above phenomenon could be explained by a stronger affinity between Cd(II) ion and $\text{Al}_2\text{O}_3/\text{MWCNTs}$ due to the electrostatic attraction and the steric hindrance effect of the formation of inner-sphere and outer-sphere complexes [55]. Meanwhile, the higher adsorption amounts were observed in preloading experiments from Fig. 8. That was because only weakly-adsorbed TCE/Cd(II) ion were desorbed and replaced by Cd(II) ion/TCE in the preloading experiments. But in simultaneous adsorption, Cd(II) ion and TCE could compete with all the adsorption sites [55].

3.6. Effect of groundwater constituents

As shown in Fig. 9, the equilibrium adsorption capacity of Cd(II) ion on $\text{Al}_2\text{O}_3/\text{MWCNTs}$ reduced with the increasing concentration of Ca^{2+} , suggesting that Ca^{2+} had a negative effect on the adsorption of Cd(II) ion. The results indicated that Ca^{2+} and Cd(II) ion could compete for the same adsorption sites due to the complexation and electrostatic forces [1]. According to the Gupta et al [43], an increasing ionic strength of solution influenced the activity coefficient of metal ions that may limit their transfer to the composite surfaces. However, the presence of HA enhanced the adsorption of Cd(II) ion. It seemed to be due to the fact that $\text{Al}_2\text{O}_3/\text{MWCNTs}$

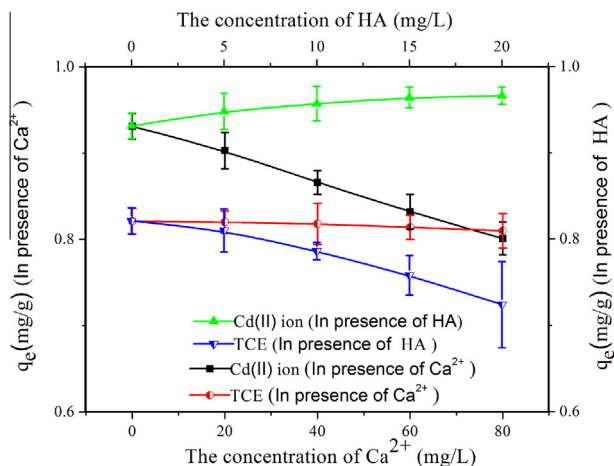


Fig. 9. Effect of groundwater constituents (CaCl_2 , HA) on the adsorbed amount of Cd(II) ion and TCE by $\text{Al}_2\text{O}_3/\text{MWCNTs}$.

Table 3

The practical application of $\text{Al}_2\text{O}_3/\text{MWCNTs}$ in ultrapure water and groundwater.

Adsorbate	Initial concentration (mg/L)	Mean adsorption capacity (mg/g)	
		Ultrapure water (pH 7.0)	Groundwater (pH 7.6)
Cd(II) ion	1.028	0.931	0.942
TCE	1.089	0.821	0.820

surface became more heterogeneous with increasing HA loading, which might be explained by the variety of functional groups introduced by HA molecules, such as carbonyl, carboxyl, aromatic and aliphatic groups [34]. These functional groups facilitated the Cd(II) ion adsorption by the electrostatic attraction. Furthermore, the rapid surface complexation of Cd(II) ion on the surface of HA particles could also contribute to the adsorption. This mechanism was represented by the following general reaction [1]:

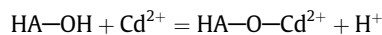


Fig. 9 also showed that the TCE adsorption capacity declined with the increasing concentration of HA. This could be explained by the fact that HA coated $\text{Al}_2\text{O}_3/\text{MWCNTs}$ were better dispersed in water forming a loosely coiled network of tubes. The coverage of $\text{Al}_2\text{O}_3/\text{MWCNTs}$ adsorption sites reduced the adsorption affinity of TCE [14]. However, the equilibrium adsorption capacity of TCE was not sensitive to the presence of Ca^{2+} . It might be resulted from the functional groups located at tube ends and defected sites on the tube sidewalls [48]. Similar results have also been observed in the case of activated carbon [13].

3.7. Application of $\text{Al}_2\text{O}_3/\text{MWCNTs}$ to groundwater samples

Table 3 shows the adsorption capacity of Cd(II) ion in synthesized groundwater was a little greater than that in ultrapure water. That was because the higher pH contributed to the Cd(II) ion adsorption (Fig. 4). Although the salinity of the synthesized groundwater hindered the adsorption of Cd(II) ion (Fig. 9), it might not be enough to cover the increase. Whereas, the adsorption capacity of TCE in synthesized groundwater was almost equal to that in ultrapure water. It was because the salinity of the synthesized groundwater slightly affected the adsorption of TCE (Fig. 9). Meanwhile, the pH would have no impact on the adsorption performance over the pH range of 7.0–9.0 (Fig. 4). From the above results, we can forecast that $\text{Al}_2\text{O}_3/\text{MWCNTs}$ exhibit good performance in simultaneous removing TCE and Cd(II) ion from groundwater.

4. Conclusions

Alumina-decorated multi-walled carbon nanotubes were successfully synthesized and used as an effective adsorbent for simultaneous removal of TCE and Cd(II) ion. The physicochemical analysis confirmed successful covalent linking of the functional groups on the $\text{Al}_2\text{O}_3/\text{MWCNTs}$ and had more active adsorption sites than MWCNTs. The BET surface area of $\text{Al}_2\text{O}_3/\text{MWCNTs}$ was much larger than MWCNTs. The $\text{Al}_2\text{O}_3/\text{MWCNTs}$ exhibited excellent adsorption performance at neutral pH for both TCE and Cd(II) ion. Both of the adsorption of TCE and Cd(II) ion by $\text{Al}_2\text{O}_3/\text{MWCNTs}$ were well fitted by the pseudo-second-order kinetic model and intraparticle diffusion model. Freundlich model was most appropriate to fit TCE adsorption, but for Cd(II) ion, the Langmuir isotherm was more appropriate. Competitive adsorption experiments showed that the adsorption of TCE and Cd(II) ion by $\text{Al}_2\text{O}_3/\text{MWCNTs}$ had insignificant impacts on each other. The presence of Ca^{2+} reduced the equilibrium adsorption capacity of Cd(II)

ion, and slightly hindered the adsorption of TCE, while the presence of HA decreased the equilibrium adsorption capacity of TCE, but facilitated the adsorption of Cd(II) ion. The adsorption mechanisms of Cd(II) ion could be summarized as the electrostatic attraction, complexation and physical properties of Al₂O₃/MWCNTs, but for TCE, would be the physical properties of Al₂O₃/MWCNTs, hydrogen bond interactions and pore-filling theory. The simulated practical application indicated that Al₂O₃/MWCNTs exhibited good behavior in removing TCE and Cd(II) ion. Thus, the results and corresponding sorption mechanisms indicate that the synthesized nano-sized Al₂O₃/MWCNTs have the potential to be employed as multi-sorbents, capable of removing both metallic and organic contaminants.

Acknowledgements

This study was financially supported by the National Natural Science Foundation of China (51479072, 50808071, 51009063, 51378190, 51409100), the Program for Changjiang Scholars and Innovative Research Team in University (IRT-13R17).

Appendix A. Supplementary data

Supplementary data associated with this article can be found, in the online version, at <http://dx.doi.org/10.1016/j.cej.2015.03.069>.

References

- [1] A. Corami, S. Mignardi, V. Ferrini, Cadmium removal from single- and multi-metal solutions by sorption on hydroxyapatite, *J. Colloid Interface Sci.* 317 (2008) 402–408.
- [2] M. Kazemipour, M. Ansari, S. Tajrobehkar, M. Majdzadeh, H.R. Kermani, Removal of lead, cadmium, zinc, and copper from industrial wastewater by carbon developed from walnut, hazelnut, almond, pistachio shell, and apricot stone, *J. Hazard. Mater.* 150 (2008) 322–327.
- [3] T.T. Tsai, C.M. Kao, J.Y. Wang, Remediation of TCE-contaminated groundwater using acid/BOF slag enhanced chemical oxidation, *Chemosphere* 83 (2011) 687–692.
- [4] V.K. Gupta, I. Ali, T.A. Saleh, A. Nayak, S. Agarwal, Chemical treatment technologies for waste-water recycling – an overview, *RSC Adv.* 2 (2012) 6380–6388.
- [5] V. Aggarwal, H. Li, S.A. Boyd, B.J. Teppen, Enhanced sorption of trichloroethene by smectite clay exchanged with Cs⁺, *Environ. Sci. Technol.* 40 (2005) 894–899.
- [6] S.-M. Lee, C. Laldawngliana, D. Tiwari, Iron oxide nano-particles-immobilized-sand material in the treatment of Cu(II), Cd(II) and Pb(II) contaminated waste waters, *Chem. Eng. J.* 195–196 (2012) 103–111.
- [7] T. Baumann, P. Fruhstorfer, T. Klein, R. Niessner, Colloid and heavy metal transport at landfill sites in direct contact with groundwater, *Water Res.* 40 (2006) 2776–2786.
- [8] R. Cossu, Groundwater contamination from landfill leachate: when appearances are deceiving!, *Waste Manage* 33 (2013) 1793–1794.
- [9] V.K. Gupta, S. Agarwal, T.A. Saleh, Synthesis and characterization of alumina-coated carbon nanotubes and their application for lead removal, *J. Hazard. Mater.* 185 (2011) 17–23.
- [10] Z. Wei, Y. Seo, Trichloroethylene (TCE) adsorption using sustainable organic mulch, *J. Hazard. Mater.* 181 (2010) 147–153.
- [11] G. Zeng, Y. Liu, L. Tang, G. Yang, Y. Pang, Y. Zhang, Y. Zhou, Z. Li, M. Li, M. Lai, X. He, Y. He, Enhancement of Cd(II) adsorption by polyacrylic acid modified magnetic mesoporous carbon, *Chem. Eng. J.* 259 (2015) 153–160.
- [12] N. Sankaramakrishnan, M. Jaiswal, N. Verma, Composite nanofloral clusters of carbon nanotubes and activated alumina: an efficient sorbent for heavy metal removal, *Chem. Eng. J.* 235 (2014) 1–9.
- [13] A. Erto, R. Andreozzi, F. Di Natale, A. Lancia, D. Musmarra, Experimental and statistical analysis of trichloroethylene adsorption onto activated carbon, *Chem. Eng. J.* 156 (2010) 353–359.
- [14] M. Ahmad, S.S. Lee, A.U. Rajapaksha, M. Vithanage, M. Zhang, J.S. Cho, S.-E. Lee, Y.S. Ok, Trichloroethylene adsorption by pine needle biochars produced at various pyrolysis temperatures, *Bioresour. Technol.* 143 (2013) 615–622.
- [15] V.K. Gupta, S. Agarwal, T.A. Saleh, Chromium removal by combining the magnetic properties of iron oxide with adsorption properties of carbon nanotubes, *Water Res.* 45 (2011) 2207–2212.
- [16] V. Gupta, T. Saleh, Sorption of pollutants by porous carbon, carbon nanotubes and fullerene – an overview, *Environ. Sci. Pollut. Res.* 20 (2013) 2828–2843.
- [17] V.K. Gupta, R. Kumar, A. Nayak, T.A. Saleh, M.A. Barakat, Adsorptive removal of dyes from aqueous solution onto carbon nanotubes: a review, *Adv. Colloid Interface Sci.* 193–194 (2013) 24–34.
- [18] K. Sun, Z. Zhang, B. Gao, Z. Wang, D. Xu, J. Jin, X. Liu, Adsorption of diuron, fluridone and norflurazon on single-walled and multi-walled carbon nanotubes, *Sci. Total Environ.* 439 (2012) 1–7.
- [19] Z.-C. Di, J. Ding, X.-J. Peng, Y.-H. Li, Z.-K. Luan, J. Liang, Chromium adsorption by aligned carbon nanotubes supported ceria nanoparticles, *Chemosphere* 62 (2006) 861–865.
- [20] J.-L. Gong, B. Wang, G.-M. Zeng, C.-P. Yang, C.-G. Niu, Q.-Y. Niu, W.-J. Zhou, Y. Liang, Removal of cationic dyes from aqueous solution using magnetic multi-wall carbon nanotube nanocomposite as adsorbent, *J. Hazard. Mater.* 164 (2009) 1517–1522.
- [21] T.A. Saleh, V.K. Gupta, Photo-catalyzed degradation of hazardous dye methyl orange by use of a composite catalyst consisting of multi-walled carbon nanotubes and titanium dioxide, *J. Colloid Interface Sci.* 371 (2012) 101–106.
- [22] T.A. Saleh, V.K. Gupta, Functionalization of tungsten oxide into MWCNT and its application for sunlight-induced degradation of rhodamine B, *J. Colloid Interface Sci.* 362 (2011) 337–344.
- [23] J.-H. Chen, D.-Q. Lu, B. Chen, P.-K. OuYang, Removal of U(VI) from aqueous solutions by using MWCNTs and chitosan modified MWCNTs, *J. Radioanal. Nucl. Chem.* 295 (2013) 2233–2241.
- [24] H. Qi, E. Mäder, J. Liu, Unique water sensors based on carbon nanotube-cellulose composites, *Sens. Actuators B: Chem.* 185 (2013) 225–230.
- [25] A. Misra, Carbon nanotubes and graphene-based chemical sensors, *Curr. Sci.* (00113891) 107 (2014) 419–429.
- [26] T.A. Saleh, S. Agarwal, V.K. Gupta, Synthesis of MWCNT/MnO₂ and their application for simultaneous oxidation of arsenite and sorption of arsenate, *Appl. Catal. B: Environ.* 106 (2011) 46–53.
- [27] T.A. Saleh, V.K. Gupta, Characterization of the chemical bonding between Al₂O₃ and nanotube in MWCNT/Al₂O₃ nanocomposite, *Curr. Nanosci.* 8 (2012) 739–743.
- [28] Y.-H. Li, S. Wang, A. Cao, D. Zhao, X. Zhang, C. Xu, Z. Luan, D. Ruan, J. Liang, D. Wu, B. Wei, Adsorption of fluoride from water by amorphous alumina supported on carbon nanotubes, *Chem. Phys. Lett.* 350 (2001) 412–416.
- [29] H. Wei, S. Deng, Q. Huang, Y. Nie, B. Wang, J. Huang, G. Yu, Regenerable granular carbon nanotubes/alumina hybrid adsorbents for diclofenac sodium and carbamazepine removal from aqueous solution, *Water Res.* 47 (2013) 4139–4147.
- [30] R.S. Amais, J.S. Ribeiro, M.G. Segatelli, I.V.P. Yoshida, P.O. Luccas, C.R.T. Tarley, Assessment of nanocomposite alumina supported on multi-wall carbon nanotubes as sorbent for on-line nickel preconcentration in water samples, *Sep. Purif. Technol.* 58 (2007) 122–128.
- [31] H. Dong, X. Guan, I.M.C. Lo, Fate of As(V)-treated nano zero-valent iron: determination of arsenic desorption potential under varying environmental conditions by phosphate extraction, *Water Res.* 46 (2012) 4071–4080.
- [32] C. Lu, Y.-L. Chung, K.-F. Chang, Adsorption of trihalomethanes from water with carbon nanotubes, *Water Res.* 39 (2005) 1183–1189.
- [33] B. Belhallaoui, A. Aziz, E.H. Elandaloussi, M.S. Ouali, L.C. De Ménorval, Succinate-bonded cellulose: a regenerable and powerful sorbent for cadmium-removal from spiked high-hardness groundwater, *J. Hazard. Mater.* 169 (2009) 831–837.
- [34] X. Zhang, M. Kah, M.T.O. Jonker, T. Hofmann, Dispersion state and humic acids concentration-dependent sorption of pyrene to carbon nanotubes, *Environ. Sci. Technol.* 46 (2012) 7166–7173.
- [35] O. Moradi, K. Zare, Adsorption of Pb(II), Cd(II) and Cu(II) ions in aqueous solution on SWCNTs and SWCNT-COOH surfaces: kinetics studies, *Fuller. Nanotub. Carbon Nanostruct.* 19 (2011) 628–652.
- [36] B. Pan, B. Xing, Adsorption mechanisms of organic chemicals on carbon nanotubes, *Environ. Sci. Technol.* 42 (2008) 9005–9013.
- [37] C.-Y. Kuo, H.-Y. Lin, Adsorption of aqueous cadmium(II) onto modified multi-walled carbon nanotubes following microwave/chemical treatment, *Desalination* 249 (2009) 792–796.
- [38] J. Xu, T. Sheng, Y. Hu, S.A. Baig, X. Lv, X. Xu, Adsorption-dechlorination of 2,4-dichlorophenol using two specified MWCNTs-stabilized Pd/Fe nanocomposites, *Chem. Eng. J.* 219 (2013) 162–173.
- [39] N.V. Perez-Aguilar, P.E. Diaz-Flores, J.R. Rangel-Mendez, The adsorption kinetics of cadmium by three different types of carbon nanotubes, *J. Colloid Interface Sci.* 364 (2011) 279–287.
- [40] M. Hadavifar, N. Bahramifar, H. Younesi, Q. Li, Adsorption of mercury ions from synthetic and real wastewater aqueous solution by functionalized multi-walled carbon nanotube with both amino and thiolated groups, *Chem. Eng. J.* 237 (2014) 217–228.
- [41] O.G. Apul, T. Karanfil, Adsorption of synthetic organic contaminants by carbon nanotubes: a critical review, *Water Res.* 68 (2015) 34–55.
- [42] X. Ren, C. Chen, M. Nagatsu, X. Wang, Carbon nanotubes as adsorbents in environmental pollution management: a review, *Chem. Eng. J.* 170 (2011) 395–410.
- [43] V.K. Gupta, A. Nayak, Cadmium removal and recovery from aqueous solutions by novel adsorbents prepared from orange peel and Fe₂O₃ nanoparticles, *Chem. Eng. J.* 180 (2012) 81–90.
- [44] V. Gupta, I. Ali, T. Saleh, M.N. Siddiqui, S. Agarwal, Chromium removal from water by activated carbon developed from waste rubber tires, *Environ. Sci. Pollut. Res.* 20 (2013) 1261–1268.
- [45] G.-C. Chen, X.-Q. Shan, Y.-S. Wang, B. Wen, Z.-G. Pei, Y.-N. Xie, T. Liu, J.J. Pignatello, Adsorption of 2,4,6-trichlorophenol by multi-walled carbon nanotubes as affected by Cu(II), *Water Res.* 43 (2009) 2409–2418.
- [46] Y. Su, A.S. Adeleye, Y. Huang, X. Sun, C. Dai, X. Zhou, Y. Zhang, A.A. Keller, Simultaneous removal of cadmium and nitrate in aqueous media by nanoscale

- zerovalent iron (nZVI) and Au doped nZVI particles, *Water Res.* 63 (2014) 102–111.
- [47] Z. Gao, T.J. Bandosz, Z. Zhao, M. Han, J. Qiu, Investigation of factors affecting adsorption of transition metals on oxidized carbon nanotubes, *J. Hazard. Mater.* 167 (2009) 357–365.
- [48] S. Li, Y. Gong, Y. Yang, C. He, L. Hu, L. Zhu, L. Sun, D. Shu, Recyclable CNTs/Fe₃O₄ magnetic nanocomposites as adsorbents to remove bisphenol A from water and their regeneration, *Chem. Eng. J.* 260 (2015) 231–239.
- [49] J. Chen, D. Zhu, C. Sun, Effect of heavy metals on the sorption of hydrophobic organic compounds to wood charcoal, *Environ. Sci. Technol.* 41 (2007) 2536–2541.
- [50] D. Robati, Pseudo-second-order kinetic equations for modeling adsorption systems for removal of lead ions using multi-walled carbon nanotube, *J. Nanostruct. Chem.* 3 (2013) 1–6.
- [51] G. Li, Z. Zhao, J. Liu, G. Jiang, Effective heavy metal removal from aqueous systems by thiol functionalized magnetic mesoporous silica, *J. Hazard. Mater.* 192 (2011) 277–283.
- [52] A. Naghizadeh, S. Nasser, S. Nazmara, Removal of trichloroethylene from water by adsorption on to multiwall carbon nanotubes, *Iran. J. Environ. Health Sci. Eng.* 8 (2011) 317–324.
- [53] O. Moradi, M. Aghaie, K. Zare, M. Monajjemi, H. Aghaie, The study of adsorption characteristics Cu²⁺ and Pb²⁺ ions onto PHEMA and P(MMA-HEMA) surfaces from aqueous single solution, *J. Hazard. Mater.* 170 (2009) 673–679.
- [54] S. Samadi, F. Khalilian, A. Tabatabaee, Synthesis, characterization and application of Cu-TiO₂/chitosan nanocomposite thin film for the removal of some heavy metals from aquatic media, *J. Nanostruct. Chem.* 4 (2014) 1–8.
- [55] W.-W. Tang, G.-M. Zeng, J.-L. Gong, Y. Liu, X.-Y. Wang, Y.-Y. Liu, Z.-F. Liu, L. Chen, X.-R. Zhang, D.-Z. Tu, Simultaneous adsorption of atrazine and Cu(II) from wastewater by magnetic multi-walled carbon nanotube, *Chem. Eng. J.* 211–212 (2012) 470–478.
- [56] H.H. Salih, C.L. Patterson, G.A. Sorial, R. Sinha, R. Krishnan, The implication of iron oxide nanoparticles on the removal of trichloroethylene by adsorption, *Chem. Eng. J.* 193–194 (2012) 422–428.
- [57] M.H. Stietiya, J.J. Wang, Zinc and cadmium adsorption to aluminum oxide nanoparticles affected by naturally occurring ligands, *J. Environ. Qual.* 43 (2014) 498–506.
- [58] L. Xiong, C. Chen, Q. Chen, J. Ni, Adsorption of Pb(II) and Cd(II) from aqueous solutions using titanate nanotubes prepared via hydrothermal method, *J. Hazard. Mater.* 189 (2011) 741–748.
- [59] H. Nishikiori, M. Furukawa, T. Fujii, Degradation of trichloroethylene using highly adsorptive allophane-TiO₂ nanocomposite, *Appl. Catal. B: Environ.* 102 (2011) 470–474.
- [60] H. Salih, C. Patterson, G. Sorial, Comparative study on the implication of three nanoparticles on the removal of trichloroethylene by adsorption-pilot and rapid small-scale column tests, *Water Air Soil Pollut.* 224 (2013) 1–11.
- [61] O.M. Kalfa, Ö. Yalçınkaya, A.R. Türker, Synthesis and characterization of nano-scale alumina on single walled carbon nanotube, *Inorg. Mater.* 45 (2009) 988–992.
- [62] S.-H. Hsieh, J.-J. Horng, C.-K. Tsai, Growth of carbon nanotube on micro-sized Al₂O₃ particle and its application to adsorption of metal ions, *J. Mater. Res.* 21 (2006) 1269–1273.
- [63] G.D. Vuković, A.D. Marinković, M. Čolić, M.Đ. Ristić, R. Aleksić, A.A. Perić-Grujić, P.S. Uskoković, Removal of cadmium from aqueous solutions by oxidized and ethylenediamine-functionalized multi-walled carbon nanotubes, *Chem. Eng. J.* 157 (2010) 238–248.
- [64] X. Wu, X. Gu, S. Lu, M. Xu, X. Zang, Z. Miao, Z. Qiu, Q. Sui, Degradation of trichloroethylene in aqueous solution by persulfate activated with citric acid chelated ferrous ion, *Chem. Eng. J.* 255 (2014) 585–592.